REPORT DOCUMENTATION PAGE

Form Approved
OMB No. 0704-0188

1. REPORT DATE *(DD-MM-YYYY)*
04/11/2013

2. REPORT TYPE
Quarterly Report

3. DATES COVERED *(From - To)*
11/06/2012 - 02/06/2013

4. TITLE AND SUBTITLE
Critical Performance Enhancement of Ultrahigh-Bandwidth Microwave Photonic Links through Nonlinear Photonic Signal Processing

5a. CONTRACT NUMBER

5b. GRANT NUMBER
N00014-12-1-0730

5c. PROGRAM ELEMENT NUMBER

6. AUTHOR(S)
Bosworth, Bryan
Wall, Walter S.
Ting, Hong-Fu
Foster, Mark A.

5d. PROJECT NUMBER

5e. TASK NUMBER

5f. WORK UNIT NUMBER

7. PERFORMING ORGANIZATION NAME(S) AND ADDRESS(ES)
The Johns Hopkins University
3400 N. Charles St.
Baltimore, MD 21218

8. PERFORMING ORGANIZATION REPORT NUMBER

9. SPONSORING/MONITORING AGENCY NAME(S) AND ADDRESS(ES)
Office of Naval Research
875 North Randolph Street
Arlington, VA 22203-1995

10. SPONSOR/MONITOR'S ACRONYM(S)
ONR

11. SPONSOR/MONITOR'S REPORT NUMBER(S)

12. DISTRIBUTION/AVAILABILITY STATEMENT
Approved for public release; distribution is unlimited.

13. SUPPLEMENTARY NOTES

14. ABSTRACT
In the second quarter of this research program we have focused on the noise performance and SFDR of the amplitude-encoded link. We have begun to investigate a sampling-based microwave photonic architecture in this quarter. Using self-phase modulation (SPM), we have implemented a first realization of this sampling-based approach where we achieve 8-dB of signal gain for a 20-GHz bandwidth link with 3.6-dB improvement in OIP3 and 3.1-dB improvement in OIP2. Additional research activities include investigation of noise correlations in four-wave mixing comb generators and the development of a compressive-sensing-based architecture for extremely rapid ultrawide-bandwidth microwave spectrum sensing.

15. SUBJECT TERMS
Microwave Photonics, Nonlinear Optics, Fiber Optics, Electro-Optics

16. SECURITY CLASSIFICATION OF: a. REPORT	b. ABSTRACT	c. THIS PAGE	17. LIMITATION OF ABSTRACT	18. NUMBER OF PAGES	19a. NAME OF RESPONSIBLE PERSON / 19b. TELEPHONE NUMBER *(Include area code)*
U	U	U	UU	9	Mark A. Foster / (410) 516-4595

ONR Quarterly Report
Grant # N00014-12-1-0730
November 06, 2012 – February 05, 2013

Johns Hopkins University

Technical Point of Contact:
Prof. Mark A. Foster
mark.foster@jhu.edu
(410) 516-4595

Administrative Point of Contact:
Mrs. Alison Wampler
awampler@jhu.edu
(410) 516-5281

Title:
Critical Performance Enhancement of Ultrahigh-Bandwidth Microwave Photonic Links through Nonlinear Photonic Signal Processing

Program Manager: Dr. Stephen A. Pappert

I. Executive Summary

In the second quarter of this research program we have focused on the noise performance and SFDR of the amplitude-encoded link. To overcome limitations from stimulated Brillouin scattering (SBS) we have begun to investigate a sampling-based microwave photonic architecture in this quarter. By making use of the nonlinear optical process of self-phase modulation (SPM), we have implemented a first realization of this sampling-based approach where we achieve 8-dB of signal gain for a 20-GHz bandwidth link with 3.6-dB improvement in OIP3 and 3.1-dB improvement in OIP2 with no power limitations from SBS. Using SPM in this sampling-based architecture provides numerous approaches to achieve distortion correction and increased signal gain while maintaining a low noise figure for the link. This parameter space will be explored in the third quarter of the research program. Additional research in the second quarter of this research program include investigation of noise correlations in the cascaded four-wave mixing (FWM) based comb generators and the development of a compressive-sensing-based architecture for extremely rapid ultrawide-bandwidth microwave spectrum sensing.

This research program currently supports two full-time graduate students pursuing their doctoral degree. In addition, two undergraduate students are currently participating in the research program and are receiving a small amount of support from this grant.

II. Research Summary

Amplitude-Encoded Microwave Photonic Link

To achieve the best noise figure for the investigated microwave photonic links it is important to avoid optical amplification within the link while maximizing the received photocurrent. Stimulated Brillouin scattering (SBS) currently limits the idler power in the four-wave mixing (FWM) interaction such that in an amplifier-less link we are thermally noise limited after photodetection due to a low received optical power. To overcome this limitation while avoiding significant signal to noise degradation we plan to employ tensioning of the highly nonlinear fiber to spread the SBS gain spectrum and thereby reduce the SBS gain [1]. As an alternative to this approach we are also currently investigating a promising new approach using self-phase modulation (SPM) in a sampling-based analog microwave photonic link. Sampling-based architectures have been shown to achieve the same performance as continuous-wave architectures while avoiding signal power limitations from SBS [2]. Additionally, of direct interest to this research program, sampling-based architectures facilitate the implementation of nonlinear photonic signal processing due to the higher peak to average power ratio of the optical signal. During this quarter we have constructed the sampling-based link depicted in Fig. 1. In this link a 24-GHz ultrafast pulsed optical source (MLL) is amplified using an erbium-doped fiber amplifier (EDFA) and then used to sample an analog microwave signal using a 20-GHz dual-output Mach-Zehnder modulator (MZM). The two modulator outputs undergo self-phase modulation (SPM) based spectral broadening in a highly-nonlinear fiber (HNLF) and are subsequently spectrally filtered with a notch filter to block the original spectral band of the sampling laser. This combination of nonlinear spectral broadening and spectral filtering yields a nonlinear power transfer function for the optical signal, which can be used for both microwave signal amplification and distortion correction. As shown in Fig. 2, we have measured the gain and distortion performance of our first realization of this approach and we achieve 8-dB of signal gain for a 20-GHz bandwidth link with a 3.6-dB improvement in OIP3 and a 3.1-dB improvement in OIP2 with no power limitation from SBS. The lack of SBS allows for maximization of the received optical power, minimizing the impact of thermal noise in the photodetector. Furthermore,

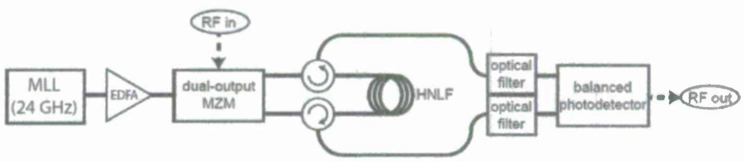

Fig. 1. Experimental setup of sampling-based microwave photonic link with self-phase modulation based enhancement and balanced detection.

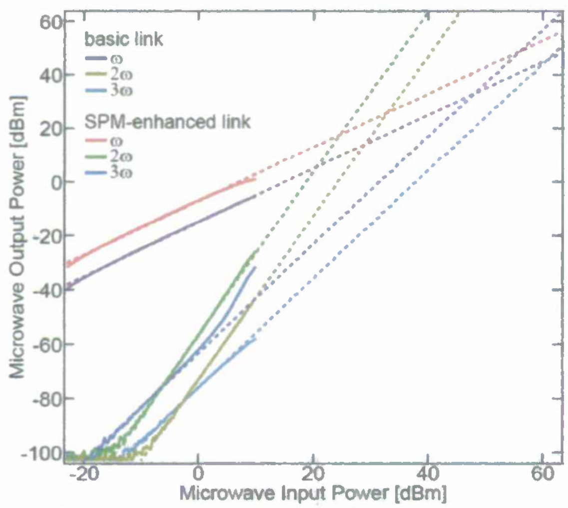

Fig. 2. Measured performance of the sampling-based link with SPM enhancement compared with a basic sampling-based link. The SPM-enhanced link shows 8-dB of signal gain, a 3.6-dB improvement in OIP3, and a 3.1-dB improvement in OIP2.

the use of the balanced detector allows for RIN cancelation and the achievement of shot-noise limited noise performance in the link. Using SPM in this sampling based architecture provides a number of approaches to achieve distortion correction and increased signal gain, including pulse pre-chirping, dispersion, spectral filtering design, and operating power. We are currently investigating this parameter space to improve upon the performance of our first generation link as well as characterizing the noise figure of the link.

Noise Transfer and Correlations in FWM-based Comb Generators

Four-wave mixing based comb generators generate an array of spectrally equidistant and phase-locked optical frequencies from one or two laser sources. Unlike mode-locked laser comb sources the spacing between comb teeth can be much wider (>100 GHz). Such combs are intriguing as efficient sources to enable highly parallel microwave photonic signal transmission and processing. However, to harness these comb sources in useful systems we must first understand their basic properties including RIN and linewidth. During this quarter we have investigated through simulation the transfer of RIN from the pump lasers to the array of newly generated frequencies in a cavity-less FWM-based comb generator. We find that the noise transfer is highly structured across the bandwidth with some teeth exhibiting amplification and some suppression of the pump laser RIN. One intriguing aspect of this noise transfer that we have identified is correlations in the noise of the comb teeth. The two pump lasers used to generate the comb have noise that is uncorrelated. However, the newly generated frequencies exhibit high degrees of correlation in their noise properties. Furthermore, the correlations vary from highly correlated to anti-correlated across the spectrum as shown in Fig. 3. These noise correlations and anti-correlations can yield significant applications for such comb sources in the realm of microwave photonics. We are currently working on verifying these simulated noise properties experimentally.

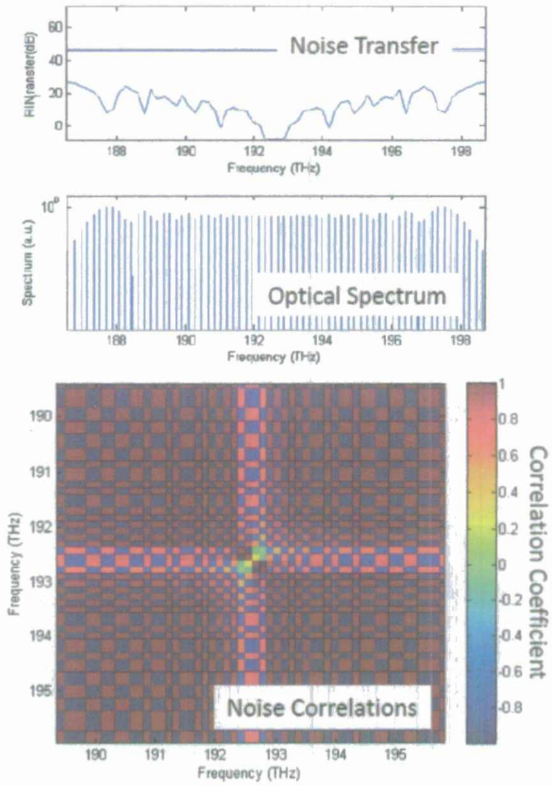

Fig. 3. Simulated noise transfer for a FWM-based comb generator. The comb is generated through cascaded FWM from two independent laser sources with uncorrelated RIN (correlation coefficient = 0). The generated comb teeth exhibit varying levels of RIN transfer from the original pump lasers. Furthermore, there are high degrees of both correlation (correlation coefficient = 1) and anticorrelation (correlation coefficient = -1) in the noise of the generated comb teeth.

Extremely Rapid Ultrawide-Bandwidth Microwave Spectrum Sensing

We have recently developed a microwave-photonic architecture that allows for compressive-sensing-based measurement of ultrawide-bandwidth microwave signals using a mode-locked laser source and applied this architecture to sparse microwave spectrum sensing. Due to their ultrashort duration mode-locked laser pulses are composed of a wide bandwidth of optical frequencies. Pulse propagation through a dispersive medium (e.g. optical fiber) will cause the ultrashort pulse to spread temporally due to group-velocity dispersion (GVD). As a result of this spreading, the instantaneous frequency of the pulse will linearly vary as a function time. Furthermore, this chirp of the pulse can be removed through propagation in the oppositely dispersive medium returning the pulse to an ultrashort duration. Our architecture makes use of these chirping dynamics to compressively sample a temporal waveform.

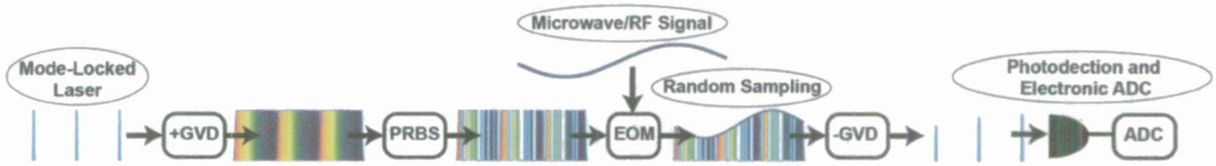

Fig. 4. Basic architecture for compressive-sensing-based ultrawide-bandwidth microwave spectrum sensing using a mode-locked laser source.

Our general approach is depicted in Fig. 4. The laser pulses are highly chirped. Subsequently the temporal profile (and consequently optical spectrum) is modulated by a high-speed pseudorandom bit pattern. This pattern serves as the random sampling pattern for compressive sensing. The RF or microwave signal under test is modulated onto the chirped and randomly structured optical waveform. Subsequently the optical pulses are compressed using dispersion compensation, which effectively integrates the randomly sampled measurement. Finally, the pulse energies are digitized with a relatively low sampling rate ADC.

The detailed hardware system for our initial implementation is shown in Fig. 5. A 90-MHz mode-locked laser (MLL) is spectrally broadened and chirped in a normal dispersion fiber (D=-38 ps/nm-km) to form a broad and flat spectral profile suitable for the sampling system. A 11.52-Gb/s pseudorandom bit sequence (PRBS) generator is used to modulate the temporal profile of the highly chirped pulses in an electro-optic modulator. This allows every pulse from the MLL to have a unique pseudorandom spectral profile. The pseudorandomly-shaped highly chirped pulses are partially compressed to increase the effective sampling rate to 30 GSamples/s. Subsequently, the microwave signal under test is sampled with this chirped random sampling source using a second electro-optic modulator. The chirped pulses

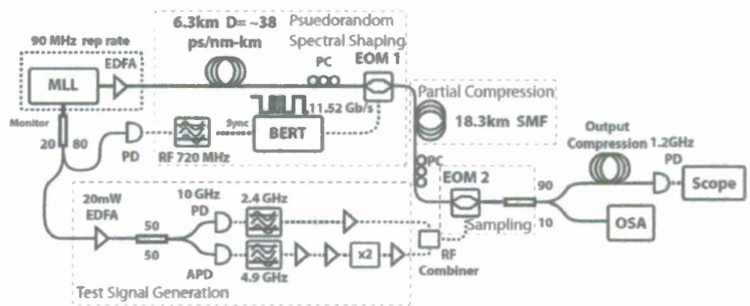

Fig. 5. Detailed hardware implementation of ultrawide bandwidth microwave spectrum sensing through compressive sensing with a mode-locked laser source.

with the encoded signals are fully compressed (to < 50 ps) in a length of anomalous dispersion fiber which effective integrates the 30 GSample/s pseudorandom measurement. Finally, the pulses are received and digitized using a relatively slow photodetector and oscilloscope. Through this system we are able to collect measurements of the microwave signal at a 90 MHz measurement rate in a single shot. Furthermore, through this approach our system architecture achieves an ultrahigh sampling rate given by the partially compressed pseudorandom bit pattern (30 GSamples/s) while requiring relatively low speed, and thereby resource efficient, digitization hardware (< 1 GHz electronic bandwidth).

An example of the rapid ultrawide-bandwidth microwave spectrum sensing enabled using this system is shown by the experimental results displayed in Fig. 6. For this measurement we use a microwave signal under test composed of two microwave tones at 2.4 GHz and 9.8 GHz. The compressive sensing system samples this signal at a rate of 30 GSamples/s and 100 pseudorandom features per laser pulse. These parameters allow for spectrum sensing up to 15 GHz with 150 MHz resolution. For sparse signals, such as the two-tone signal under test, compressive sensing allows for reconstruction of the microwave spectrum with much less than the typically required 100 measurements. The experimental results shown in Fig. 6 are generated using only 25 measurements taken in a single shot (no averaging). Given the 90 MHz measurement acquisition rate these 25 measurements are collected in only 278 ns. Furthermore, we are able to reconstruct spectra with microwave signals up to 15 GHz using a < 1 GHz digitization bandwidth and an 11.5 Gb/s pattern generator. With increased partial compression and temporal multiplexing the measurement rate can readily be increased to > 1 GHz (allowing for a ~ 10 ns total measurement time) and the sampling rate can be increased to > 80 GSamples/s (allowing for reconstruction of microwave spectra beyond 40 GHz). The rapid measurement rate of this sensing system is particularly promising for spectrum sensing of rapidly varying (i.e. temporally dynamic) sparse microwave signals.

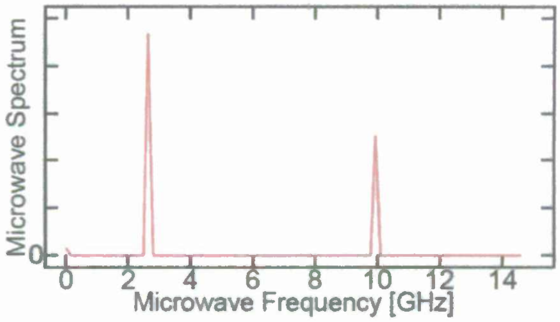

Fig. 6. Experimentally reconstructed microwave spectrum of a two-tone test signal (2.4 GHz and 9.8 GHz) using the developed compressive sensing architecture. The measurements necessary to reconstruct this spectrum are collected in under 300 ns using < 1-GHz-bandwidth digitization hardware.

III. Management Summary

Two graduate students, Hong-Fu Ting and Bryan Bosworth, are currently employed to carry out this research program. In addition, two undergraduate students, Jasper Stroud and Mitchell Sacks, are currently assisting with the research program and their work is supported by the funding. All of the student's progress and research directions are overseen by Prof. Mark Foster through weekly research meetings and hands-on experimental assistance. The research team has made very good progress towards the completion of the tasks as depicted graphically in Fig. 4. The phase-encoded tasks have been delayed while we focus on the amplitude-encoded architecture. Consequently the amplitude-encoded tasks are ahead of the original schedule. The tasks descriptions are detailed below the figure for reference.

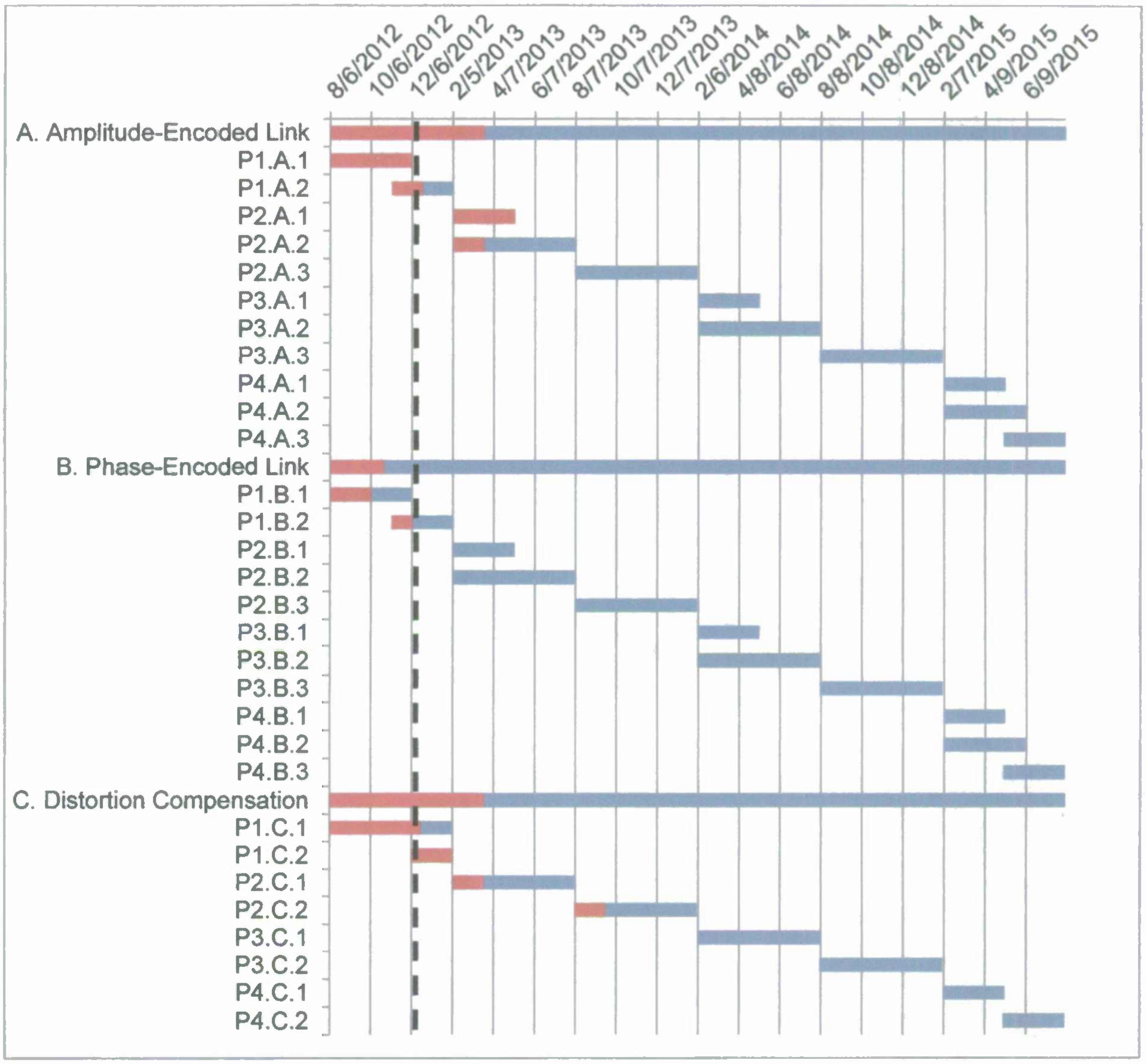

Figure 4. Anticipated task schedule and current progress towards task completion. The black dotted line indicates the current date.

Project Schedule and Milestones

The anticipated schedule of the events, milestones, and deliverables are detailed below by period.

Period 1 (months 1-6)

Milestones:

1) Fully characterized 14-GHz bandwidth amplitude-encoded link and with 9-dB FWM gain enhancement.
2) Phase-encoded link with 10-GHz bandwidth and 6-dB FWM gain enhancement.

Task A. Amplitude-Encoded Link

P1.A.1. Generate a pair of cascaded FWM spectra using the two output of the MZM.

P1.A.2. Characterize the noise figure of the amplitude encoded link with 9-dB gain enhancement.

Task B. Phase-Encoded Link

P1.B.1. Implement local oscillator generation and FWM phase multiplication.

P1.B.2. Demonstrate 6-dB of FWM gain enhancement in the phase-encoded link.

Task C. Distortion Compensation

P1.C.1. Characterize the SFDR of the amplitude encoded link with 9-dB gain enhancement.

P1.C.2. Characterize the power transfer characteristics for the generated wavelength channels in the cascaded FWM interaction.

Period 2 (months 7-18)

Milestones:

1) Amplitude-encoded link with 20-GHz bandwidth, >16 dB FWM gain enhancement, and <10 dB noise figure.
2) Phase-encoded link with 20-GHz bandwidth, >10 dB FWM gain enhancement, and <10 dB noise figure.
3) Distortion compensation capable of 10-dB improvement in SFDR.

Task A. Amplitude-Encoded Link

P2.A.1. Demonstrate a 20-GHz amplitude-encoded link with FWM gain enhancement.

P2.A.2. Demonstrate > 16 dB of FWM gain enhancement in the amplitude-encoded link.

P2.A.3. Demonstrate < 10 dB noise figure in the amplitude-encoded link.

Task B. Phase-Encoded Link

P2.B.1. Demonstrate a 20-GHz phase-encoded link with FWM gain enhancement.

P2.B.2. Demonstrate >10 dB FWM gain enhancement in phase-encoded link.

P2.B.3. Demonstrate < 10 dB noise figure in the phase-encoded link.

Task C. Distortion Compensation

P2.C.1. Characterize the SFDR of the demonstrated links.

P2.C.2. Demonstrate 10-dB SFDR improvement using transfer function synthesis.

Period 3 (months 19-30)

Milestones:

1) Amplitude-encoded link with 30-GHz bandwidth, >23 dB FWM gain enhancement, and <8 dB noise figure.
2) Phase-encoded link with 30-GHz bandwidth, >16 dB FWM gain enhancement, and <8 dB noise figure.
3) Distortion compensation capable of 20-dB improvement in SFDR.

Task A. Amplitude-Encoded Link

P3.A.1. Demonstrate a 30-GHz amplitude-encoded link with FWM gain enhancement.

P3.A.2. Demonstrate > 23 dB of FWM gain enhancement in the amplitude-encoded link.

P3.A.3. Demonstrate < 8 dB noise figure in the amplitude-encoded link.

Task B. Phase-Encoded Link

P3.B.1. Demonstrate a 30-GHz phase-encoded link with FWM gain enhancement.

P3.B.2. Demonstrate >16 dB FWM gain enhancement in phase-encoded link.

P3.B.2. Demonstrate < 8 dB noise figure in the phase-encoded link.

Task C. Distortion Compensation

P3.C.1. Characterize the SFDR of the demonstrated links.

P3.C.2. Demonstrate 20-dB SFDR improvement using transfer function synthesis.

Period 4 (months 31-36)

Milestones:

1) Amplitude-encoded link with 40-GHz bandwidth, >30 dB FWM gain enhancement, and <6 dB noise figure.
2) Phase-encoded link with 40-GHz bandwidth, >23 dB FWM gain enhancement, and <6 dB noise figure.
3) Distortion compensation capable of 30-dB improvement in SFDR.

Task A. Amplitude-Encoded Link

P4.A.1. Demonstrate a 40-GHz amplitude-encoded link with FWM gain enhancement.

P4.A.2. Demonstrate > 30 dB of FWM gain enhancement in the amplitude-encoded link.

P4.A.3. Demonstrate < 6 dB noise figure in the amplitude-encoded link.

Task B. Phase-Encoded Link

P4.B.1. Demonstrate a 40-GHz phase-encoded link with FWM gain enhancement.

P4.B.2. Demonstrate >23 dB FWM gain enhancement in phase-encoded link.

P4.B.3. Demonstrate < 6 dB noise figure in the phase-encoded link.

Task C. Distortion Compensation

P4.C.1. Characterize the SFDR of the demonstrated links.

P4.C.2. Demonstrate 30-dB SFDR improvement using transfer function synthesis.

IV. Financial Status Report

We are currently spending at the anticipated rate. The deviation from planned spending depicted in Fig. 5 is due to a large capital equipment purchase that has arrived in the lab but has not yet been invoiced. We are spending at the planned monthly rate other than this impending capital equipment charge, which should officially post in the next quarter.

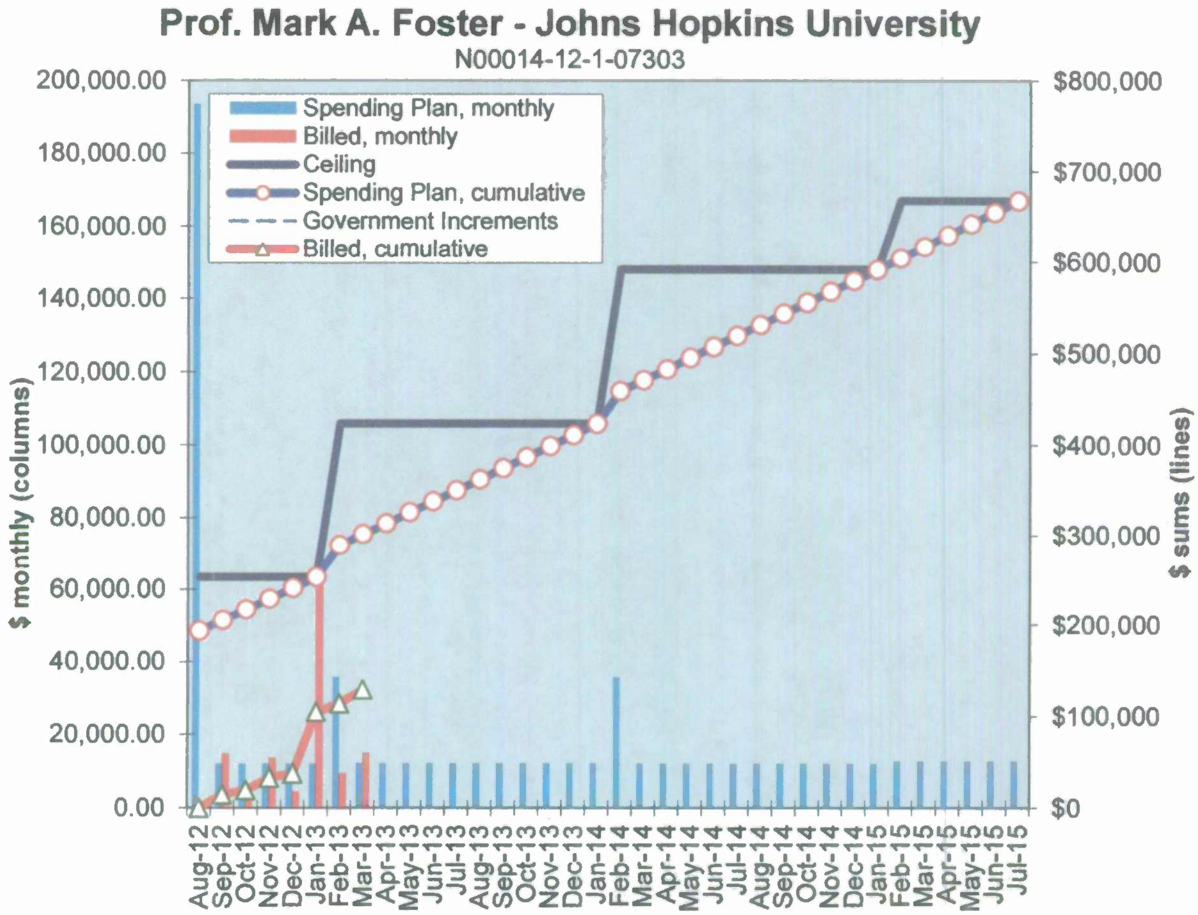

Figure 5. Graphical depiction of planned spending and current financial status.